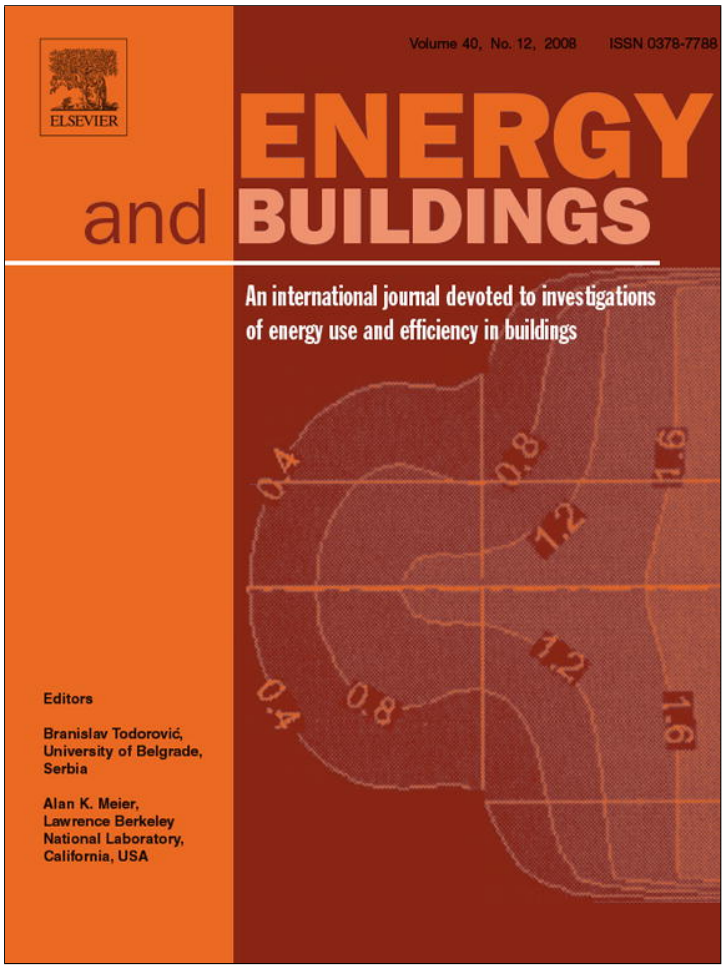

Energy and Buildings 40 (2008) 2196–2206

Contents lists available at ScienceDirect

Energy and Buildings

journal homepage: www.elsevier.com/locate/enbuild

A laboratory experiment on natural ventilation through a roof cavity for reduction of solar heat gain

L. Susanti [a,*], H. Homma [b], H. Matsumoto [b], Y. Suzuki [c], M. Shimizu [d]

[a] Environment and Life Engineering, Toyohashi University of Technology, Tenpakucho, Hibariga-oka 1-1, Toyohashi 441-8580, Japan
[b] Architecture and Civil Engineering, Toyohashi University of Technology, Tenpakucho, Hibariga-oka 1-1, Toyohashi, 441-8580, Japan
[c] Kakegawa Technical School, Kakegawa, Japan
[d] Sala-House Co., Ltd., Shirakawacho 100, Toyohashi, Japan

ARTICLE INFO

Article history:
Received 17 August 2007
Received in revised form 3 June 2008
Accepted 17 June 2008

Keywords:
Cavity
Natural ventilation
Air temperature
Air velocity
Resistance

ABSTRACT

The study targets the reduction of roof solar heat gain through the use of natural ventilation in a roof cavity. This study is mainly concerned with factory buildings. Experimental outcomes were obtained from an inclined cavity model which was heated on the upper surface to mimic solar radiation on a roof. The dimensions of the cavity were 4882 mm × 400 mm × 78 mm. The two opposing smallest sides were allotted as the inlet and outlet, and narrowed to simulate resistance of the air flow in practical applications. Temperature and velocity measuring facilities were prepared in the experimental model. A number of measurements were carried out by varying the combinations of different heat production, inclination angles, and opening ratios. It was found that resistance to heat and air flow in the cavity was strongly influenced by the opening size. When the Reynolds number was examined, it showed that the flow belonged to the laminar region. The average velocity reached to 0.25 m/s at the highest in the examined cases. In other words, the cavity air was turned over 184 times in an hour. Natural ventilation in the roof cavity seemed to be effectively applicable to solar incidence discharges in factory buildings.

1. Introduction

During the rapid industrial development period of Southeast Asia several decades past, many factories were built with corrugated asbestos cement boards. The typical structure was comprised of a single-story building of relatively low height with a widely spread roof. In such a building, the heat transfer characteristics of the roof have an exclusive influence on the thermal environment as well as the thermal load beneath. In particular, solar irradiation on the roof outweighs the cooling load substantially, making the workspace below unbearably hot, which in turn causes a reduction in work efficiency and precision.

These factory buildings have now become aged and decayed, requiring expensive maintenance and repair work. Instead of repairing the roofs, roofers are developing measures to completely cover them with thin, folded metal plates. When an old single roof is covered in this way, a cavity is formed between it and the new cover. If this cavity could be ventilated, it would reduce the penetration of solar radiation and thus reduce the temperature and cooling load of the working space. This prevention method is also more practical in an economic sense when considering the initial investment against long-term expenses.

Considerable studies have been devoted to solar energy utilization of the roof structure. Khedari et al. [1] conducted research on a solar chimney attached to the roof, widely known as a roof solar collector (RSC), which enhanced the natural ventilation of the space beneath. Some configurations of RSCs made from different materials have been investigated for application to residential houses. It has been found that an RSC constructed of gypsum board performed better than plywood in resisting heat loss in order to maximize ventilation rates. Moreover, in order to optimize natural ventilation, the length of the RSC should be shortened to the order of 1 m, inclined at 30° with an air gap size of 14 cm. Khedari et al. [2] and Hirunlabh et al. [3] implemented different types of solar collectors and found that when using the solar collectors alone, the potential for induction of sufficient air flow in order to satisfy occupants' comfort in a hot climate was negligible. To improve the air speed in the test room, two roof solar collectors combined with three configurations of solar chimneys were installed and subsequently investigated by Khedari et al. [4]. They observed that induced air motion of about 0.04 m/s at 1 m

* Corresponding author. Tel.: +62 751 7050 819; fax: +62 751 72566.
E-mail addresses: onna158@yahoo.com, lusi@einstein.tutrp.tut.ac.jp, susantilusi@gmail.com (L. Susanti).

0378-7788/$ – see front matter © 2008 Elsevier B.V. All rights reserved.
doi:10.1016/j.enbuild.2008.06.016

above the living room floor could not ensure the occupants' comfort with indoor temperature of 35–37 °C. Therefore, a higher velocity was needed. Two roof solar collectors known as the single pass RSC and the double pass RSC were analyzed and compared by Zhai et al. [5]. It was found that the performance of the double pass RSC was superior to its single pass RSC counterpart for both inducing natural ventilation in the summer and pre-heating air in the winter.

In an attempt to cool down photovoltaic cells, Moshfegh and Sandberg [6] investigated a buoyancy-driven air flow behind photovoltaic panels. The design principle of the system had a similar concept as that of the solar chimney with uniform heat on the sun-facing wall, while the remaining walls were unheated. The experimental outcomes exhibited that, with a heat flux equivalent to 200 W/m^2 or greater on the surface of the panel, the amount of heat transferred to other unheated walls by radiation could be reduced by up to 30%, depending on the surrounding wall emissivity. Using the same heat flux, Sandberg and Moshfegh [7] demonstrated that ventilation flow rates decreased in relation to the inclination angles. Meanwhile Zhai et al. [8] found that a maximum natural ventilation flow rate could be created with an optimum inclination angle for solar air collection was 45°.

In another study conducted by Manzan and Saro [9], the lower surface of the cavity was kept damp and the external air was cooled by flowing over it, thus, protecting the internal part of the roof from solar gains and reducing the temperature. The thermal performance of an inclined and ventilated roof was also theoretically investigated by Ciampi et al. [10]; demonstrating that energy conservation of over 30% could be achieved in the summer compared to the energy expense of a non-ventilated structure.

In most of the existing roof cavity ventilation studies, their object was to aid the ventilation of the occupied space of a dwelling with a relatively short roof cavity. The present study distinguished from other literatures where the model was aimed for sizeable length of a factory roof and the ventilation circuit was isolated from the working space. Solar heat transmission plays dominant effect on the thermal environment and cooling load in a factory building, and at the same time a large inclined roof arose considerable natural ventilation force of buoyancy to dissipate solar heat before it is transmitted into the working spaces below.

This paper examined experimentally the behavior of natural ventilation in a roof cavity using an open-ended inclined cavity model heated from above in a laboratory. It was difficult to satisfy the similarity laws of flow and heat transfer simultaneously in the present experiment. So the full-scale experiment was planned with a length of 4.882 m. In most of the roof cavity natural ventilation experiments, the lengths of the cavity were limited to 2 m [1–6,11–17]. The present experiment intended to clarify the friction resistance of the flow along the cavity wall, assuming that resistance by deformation along the flow channel could be decided from existing publications. If the friction resistance was known, then the resistance of a longer cavity could also be estimated from this result. This experiment was aimed to attain practical data for numerical simulation of the heat dissipation effect of cavity roofs in the next stage of this study.

With regard to the practical applications of roof cavities ventilation in factories, the inlet or outlet openings of a cavity are usually covered with a grid or a net for protection from threats such as rainwater, insects, birds, or falling leaves. Structural elements such as rafters also exist in the cavity. These obstructions shall be treated as the deformation resistance of air flow.

To cope with resistance in a roof cavity, the openings of the cavity in our experimental model were restricted by several opening configurations at the inlet or outlet. Investigation made by Katsoulas et al. [18] on the effect of vent openings and insect screens on greenhouse ventilation, reported that the use of anti-aphid screens in vent openings caused a 33% reduction in greenhouse ventilation rate. The experiment carried out by Nada and Moawed [19] demonstrated that heat transfer rates in an enclosure heated from bottom with different venting arrangements increased as the opening ratio (OR) of the outlet slots increased at an inclination angles range between 0° and 90°. However, the effect of heat transfer decreased with the opening ratio as the inclination increased from 90° to 180°, in this case the heated surface was located at the top.

Therefore in the present experiment, the resultant flows of heat and air were investigated by gauging and observing the influences of opening restrictions and their distributions on the behavior of heat and air flow in the cavity.

2. Experimental arrangement

2.1. Experimental set-up

The experimental study was carried out in a laboratory to examine the detailed behavior of air in a roof cavity under steady conditions. The experimental model had a simple rectangular duct section with a length of 4882 mm, a width of 400 mm, and a depth of 78 mm. The two smallest opposing sides were open to the laboratory as the air inlet and outlet. They were located at the high and low positions of the duct. The other sides were constructed of plywood 12 mm in thickness and then covered with foamed polystyrene thermal insulation boards of a thickness of 50 mm. A photograph of the experimental model and a sectional diagram of it are displayed in Figs. 1 and 2.

Six electric heating plates were buried in the upper structure of the model along its length. Each of the plates was connected to a voltage controller (Toshiba SK 110 AC 100 V) and the power input was adjusted individually for each plate. The upper and lower sides of the heating plates were covered with rubber sheets of a thickness of 5 mm in order to measure the heat flux across them. The insulation board above the heater directed the generated heat to the lower side. The lower surface of the rubber sheet was covered with aluminum foil in order to reduce radiation from the surface. 18 T-type thermocouples were inlaid between the rubber sheet and the aluminum foil to measure the surface temperature distribution along the centreline.

The internal surfaces of the other three sides were coated with mud black paint. 18 T-type thermocouples were also attached in order to measure the lower surface temperatures at corresponding

Fig. 1. Photograph of cavity model.

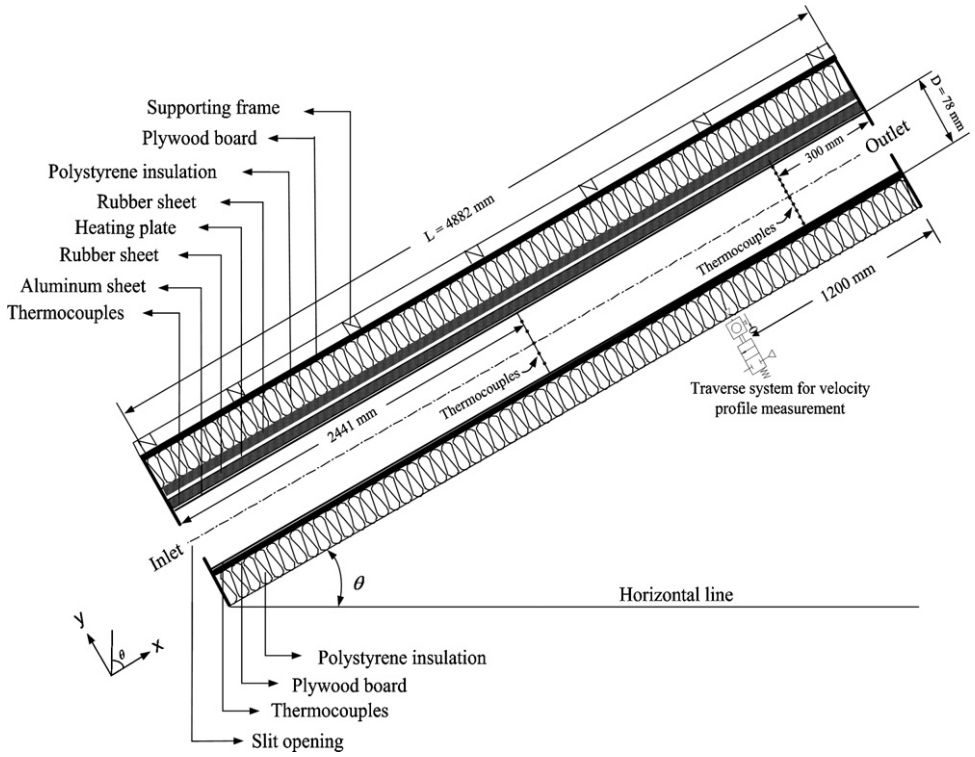

Fig. 2. Sectional diagram of cavity model.

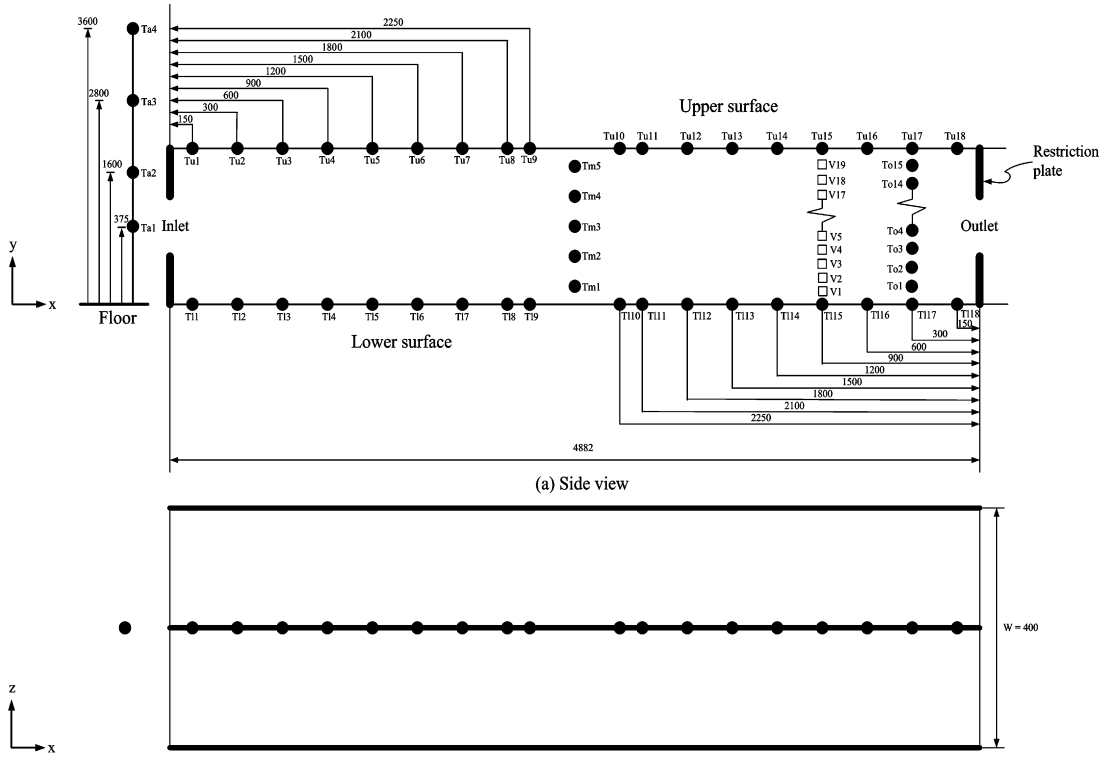

Fig. 3. Position of thermocouples and velocity sensors.

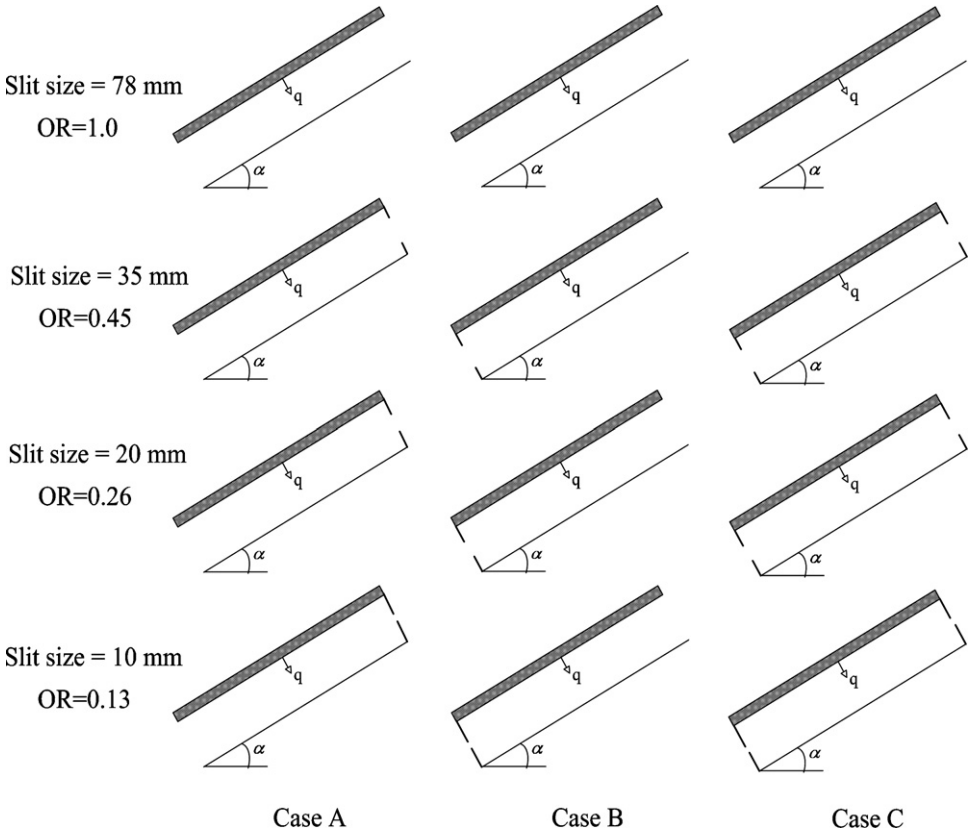

Fig. 4. Opening ratios and experimental cases.

positions to the upper surface. The thermocouple wires were flattened to a thickness of 0.1 mm to make the surfaces as smooth as possible. Heat loss through the upper and lower structures was estimated from measured temperature distributions across the plates.

At a distance of 300 mm from the outlet, 15 T-type thermocouples were arranged across the cavity at the centre to measure the temperature profile of the outgoing air. The other five thermocouples were placed in the middle of the cavity length in order to measure the air temperature rise in this location. The ambient temperature was measured at positions where the air temperatures would not be disturbed by warm air escaping from the cavity. All the thermocouples output signals were acquired with a multi-channel data logger (TR 2724; Advantest Co. Ltd.) with a precision of 0.1 °C and sent to a PC for further data processing.

A velocity profile was measured on the centreline at a distance of 1200 mm from the outlet. It was assumed that the velocity profile was most representative at this location. An anemometer probe (Model 6201, Kanomax) was attached to a traverse system, and the velocity profile was read at 19 locations spaced at 4 mm apart across the cavity. The anemometer probe had a heated sphere with a diameter of 2.5 mm. The accuracy was 0.02 m/s according to the manufacturer's manual. The results of the velocity measurement were transferred to the PC. Positions of the thermocouples and air velocity probe are shown in Fig. 3.

The examined inclination angles were set to 20° and 30° from the horizontal line. These were the slopes often used for factory roof construction. The examined heat productions were 150, 100, 75, and 50 W/m^2. These values were selected considering that the sol–air temperature increased from an ambient temperature by 36 °C at the highest, and the top cover of the cavity roof was made of a thin metal plate.

To cope with resistances against air flow in the cavity, both the inlet and outlet were restricted with aluminum plates leaving slit-type openings with sizes of 78, 35, 20, and 10 mm, respectively, located at the centre horizontally. The corresponding opening ratios were 1.0, 0.45, 0.26, and 0.13, respectively. Three combinations of opening restrictions were examined which were shown in Fig. 4. Case A represented a restriction at the outlet while the inlet was fully open. In case B, the inlet was restricted while the outlet was fully open. In case C, both the inlet and outlet were restricted equally. An opening ratio of 1.0 was used as a reference for all the cases.

The entire cavity assembly was supported by a framework which was suspended from the laboratory ceiling. The cavity could be adjusted to a required angle in the frame. The inlet of the cavity was located 375 mm above the laboratory floor.

The experiment was conducted in a laboratory of a height of 6.5 m and a width of 6.0 m, with a tilted roof of heights of 4.5–5.5 m. The laboratory was thermally well insulated for protection from outdoor temperature fluctuations.

2.2. Experimental procedure

When the cavity was set to a required angle, the experiment was carried out with different levels of heat production and opening combinations. After changing the configuration, the input power was adjusted to attain an equivalent heat flux in the six heaters. The model was allowed to run at least 20 h until a thermally steady condition was achieved. Using a transient heat transfer calculation, it was estimated that the heat flux reached 99% of the newly changed heat flux in 20 h. It was confirmed that temperatures did not fluctuate more than 0.1 °C before each measurement. When a steady-state condition was achieved, the

temperatures and the velocities were recorded. The experiments consisted of 3 and 10 sequences of test runs for velocity and temperature measurement, respectively. Experiments with some of the configurations could not be performed because the heater temperature rose too high either when the heat flux was high, the openings were small, or the tilting angle was low.

3. Experimental results

3.1. Surface temperature distributions

Experiments with all the conditions took several months. During these months the daily laboratory temperatures changed. Thus in the following discourse, all temperatures were referred to the average laboratory temperatures of respective measurements, and subsequent increases were discussed.

Fig. 5(a), (b), and (c) shows the temperature distributions along the centreline of upper and lower surfaces in the cavity for cases A, B, and C, respectively. During this experiment, the cavity was tilted at an angle of 30°, the heat production was set at 100 W/m^2, and the opening ratios were changed to 1.0, 0.45, 0.26, and 0.13.

In general, temperatures on both the upper and lower surfaces increased depending on distances from the inlet. This demonstrated that the stack effect worked well in the cavity. But the increases were not linear along the cavity length, particularly on the upper surface. The temperatures on the upper surface

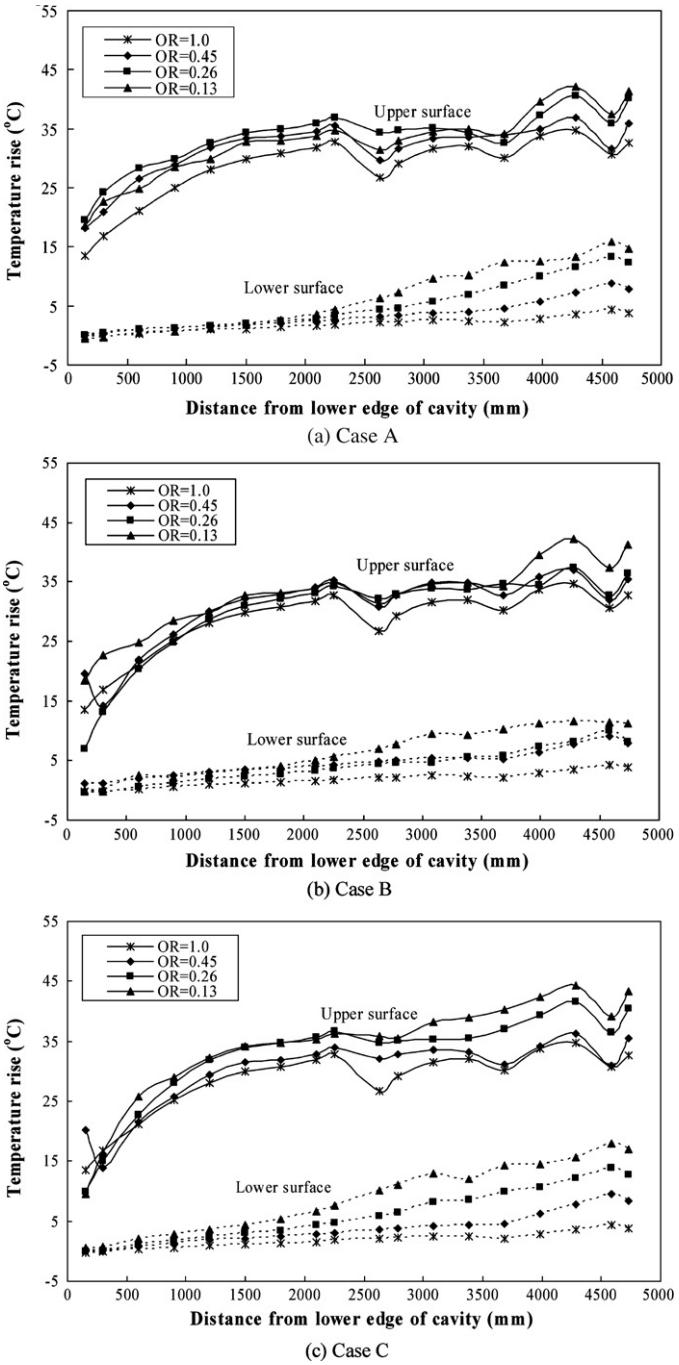

Fig. 5. Upper and lower surface temperature distributions.

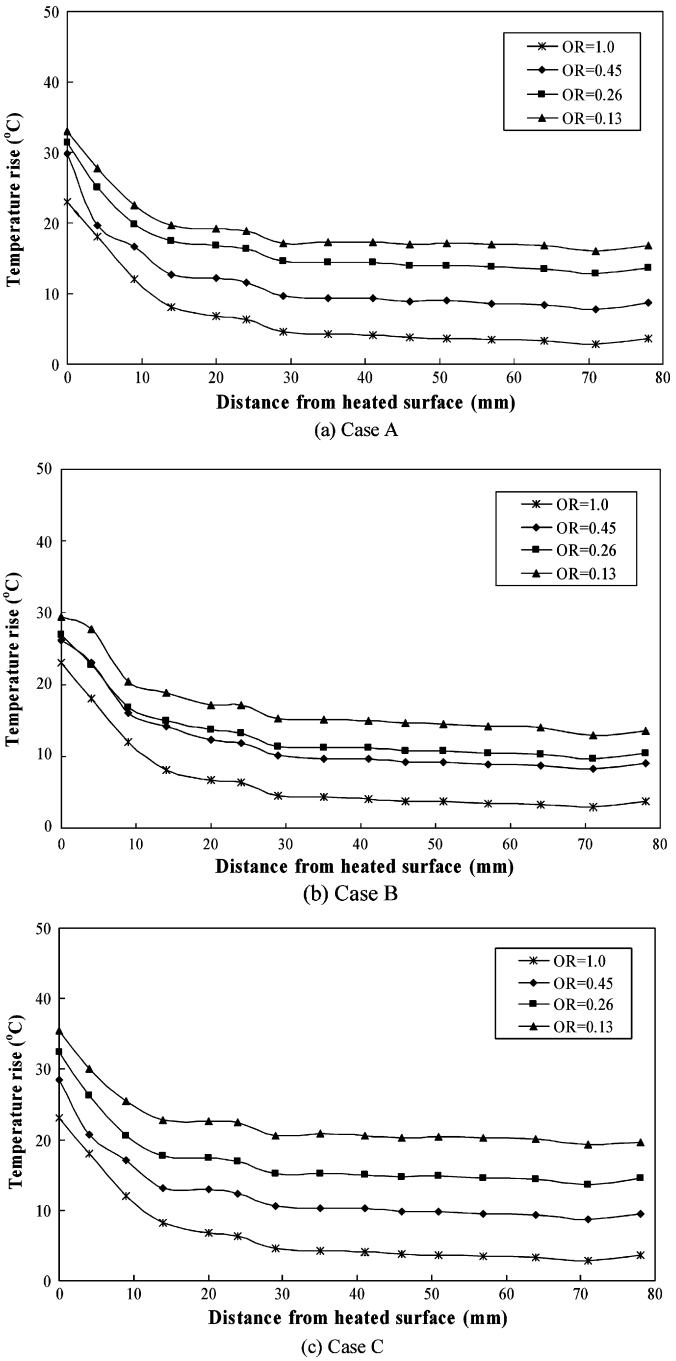

Fig. 6. Temperature profiles across the cavity.

increased rapidly within the lower one-third of the cavity. Beyond this region, the temperature increase was gradual but irregular, and there were also distinct temperature drops at several positions.

The temperature drop at a measuring point of 2632 mm from the inlet was probably caused by the discontinuity of heaters at this location. However, the reason for the temperature drop near the outlet remained unknown. In the case of a vertical channel studied by Chen et al. [15] and Sandberg and Moshfegh [16], it was shown that the drop in the heated surface temperatures could only be caused by an increase in the local heat transfer coefficient. This increase was possibly caused by a transition between the laminar flow and turbulent flow or the degree of turbulence.

On the lower surface, generally, temperatures rose almost linearly with the distance from the inlet. The rise of temperature was small in the region near the inlet but steady increases were noticed as the position gradually neared the outlet. In practical situations, the temperature distribution on the lower surface plays an important role to dictate the portion of heat transmitted to the space below. In outlet restricted cases of A and C, the increase in exit temperatures were larger compared to those of outlet restricted case of B, because in the former two, the upward motion of hot air was blocked by the restriction. This caused accumulation of hot air in this area, resulting in an increase in surface temperatures. Most importantly, the increments of temperature were much larger when the restrictions were tighter.

3.2. Temperature profiles across cavity

Fig. 6(a)–(c) shows the air temperature profiles across the cavity at a measuring position of 300 mm from the outlet with the cavity tilted at an angle of 30°, a heat production of 100 W/m^2, and opening ratios of 1.0, 0.45, 0.26, and 0.13.

All temperature profiles indicated that the highest temperature appeared at the measuring position nearest to the heated upper surface. Temperatures decreased rapidly as distance increased from the heated surface. This decrease gradient became small in the region near the unheated lower surface. The air that was in closer vicinity to the heated surface had lower density than that of its surroundings. Thus, the air near the upper surface moved quickly while relatively heavy air near the lower surface moved slowly. The temperature at the position nearest to the unheated surface rose slightly. This was due to heat transferred from the heated upper surface to the lower unheated surface via radiation. Results of temperature profiles in this study satisfactorily correlated with corresponding laboratory results observed by other researchers [6,12,15].

Fig. 6 also showed that an increase in restriction increased the temperature rise in all cases. For the same opening ratio, case B exhibited a smaller temperature rise than that of cases A and C.

3.3. Velocity profiles across cavity

The velocity profiles shown in Fig. 7(a), (b), and (c), respectively, for cases A, B, and C, were obtained when the heat production was kept at 100 W/m^2, the cavity was tilted at an inclination angle of 30°, and the inlet and/or outlet opening ratios were changed to 1.0, 0.45, 0, 26, and 0.13, respectively. A fast upward air stream occurred at the region near the heated upper surface, and this velocity was reduced as the position moved closer to the unheated surface. The peak of velocity was found at a distance of around 8 mm from the heated surface. For OR 1.0, the highest air velocity reached 0.32 m/s.

This figure also indicates that the opening ratios definitely dictated the velocity. The average velocity was 0.25 m/s when both openings were OR 1.0, but decreased to 0.09, 0.01, and 0.05 m/s, respectively, for cases A, B, and C when the openings were restricted to OR 0.13.

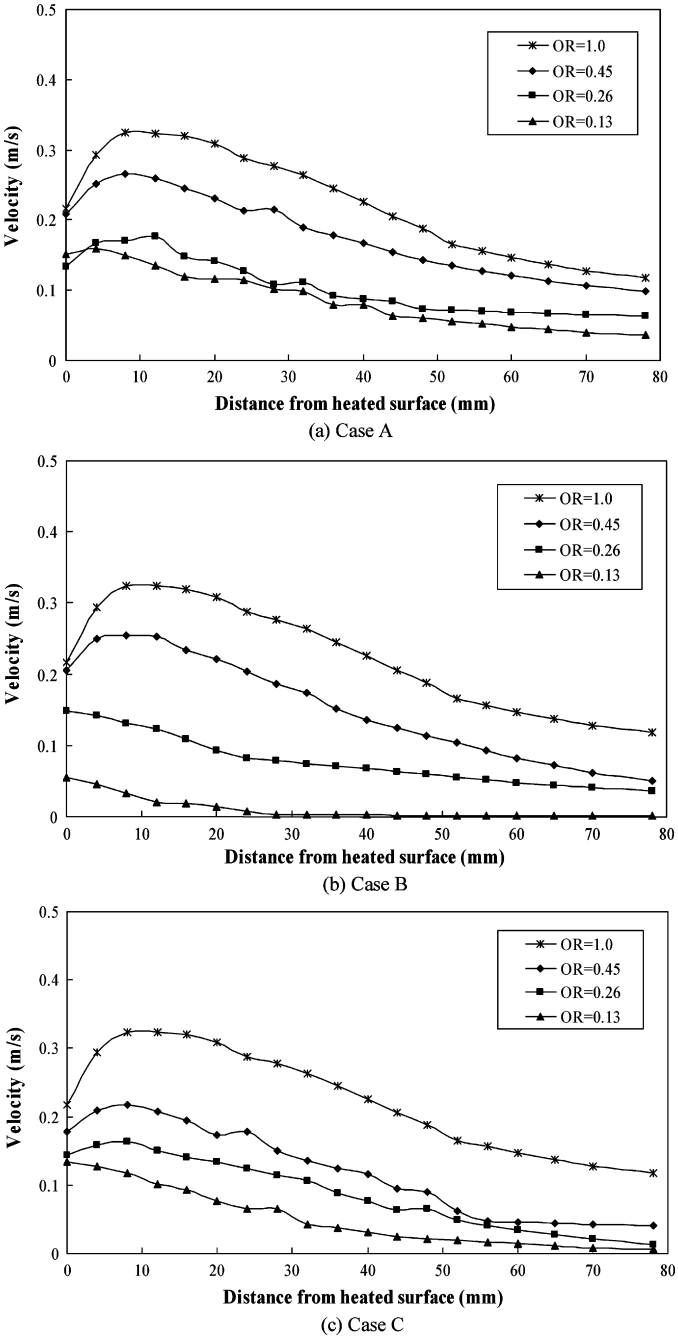

Fig. 7. Velocity profiles across the cavity.

3.4. Effect of heat production

Fig. 8(a) and (b) illustrates the effects of various degrees of heat production on velocity and temperature profiles for case C when both the inlet and outlet openings were restricted to OR 0.45 equally and the cavity was tilted at an angle of 30°. The rise in temperatures and induced air velocity profiles were strongly influenced by the heat produced. The greater the heat produced, the higher the rise in temperature and the faster the air velocity. Since a greater heat production caused higher air temperature in the cavity, a higher stack pressure for driving air flow was also

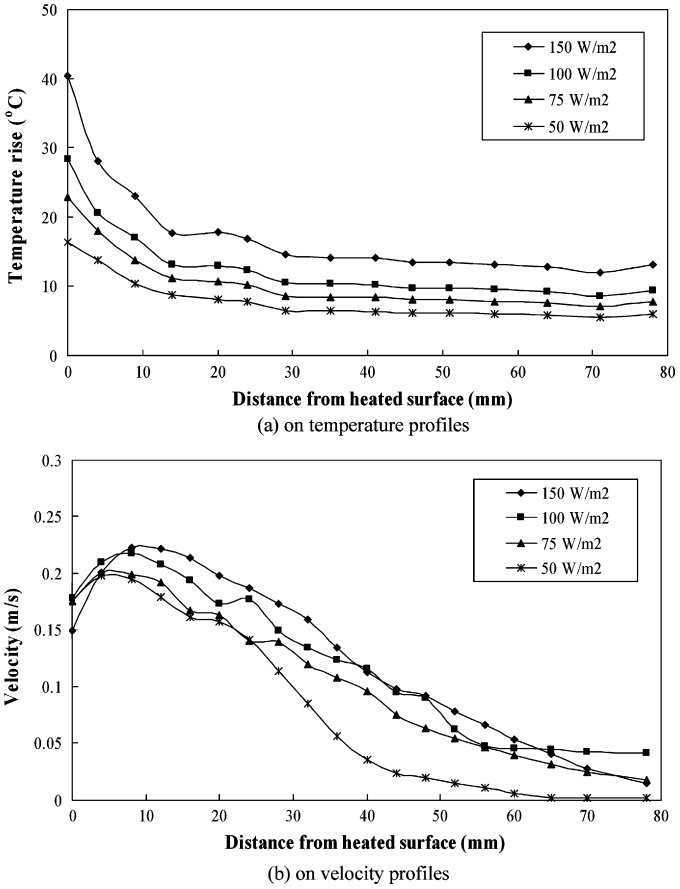

Fig. 8. Effect of different heat production (case C, OR 0.45).

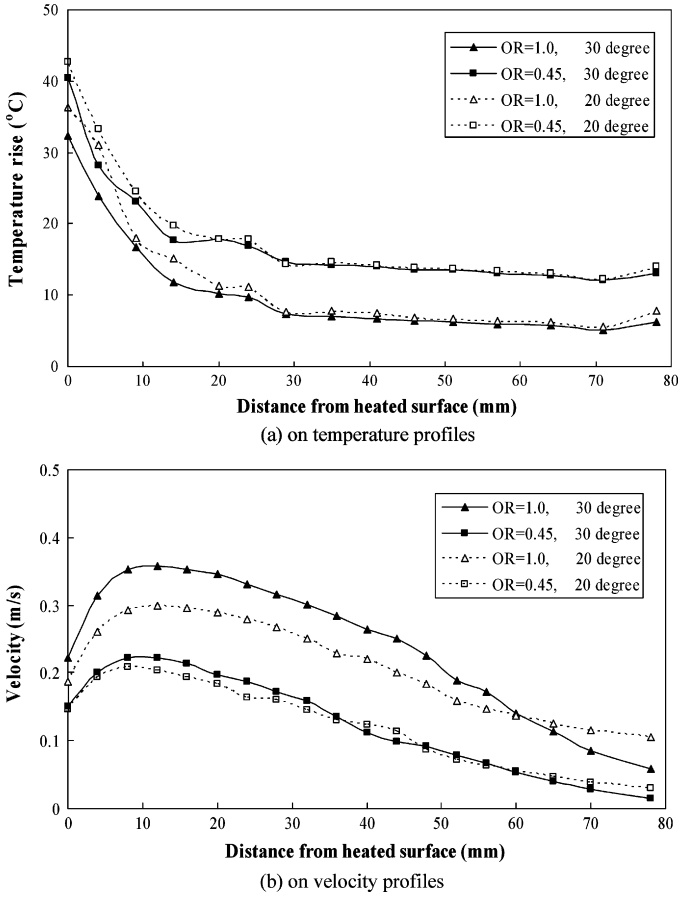

Fig. 9. Effect of inclination angles.

caused. In practice, strong cavity ventilation coincides with the time of strong solar radiation on a roof. This is beneficial for the reduction of cooling loads during peak daytime hours in a summer season.

3.5. Effect of inclination angles

Fig. 9(a) and (b) gives the temperature and velocity profiles of case C when the heat production was kept at 150 W/m^2, the opening ratios were 1.0 and 0.45 and the angles were 30° and 20°. Generally for every opening ratio, the temperature rise decreased and the velocity increased as the inclination increased. This indicated that natural ventilation was promoted according to the inclination of the roof. Subsequently, a steep inclination was recommended [16,11,17,20].

Since similar profiles for temperature rise and velocity were found for the other configurations in the experiment, no more details were given for such profiles in this paper hereafter. Thus

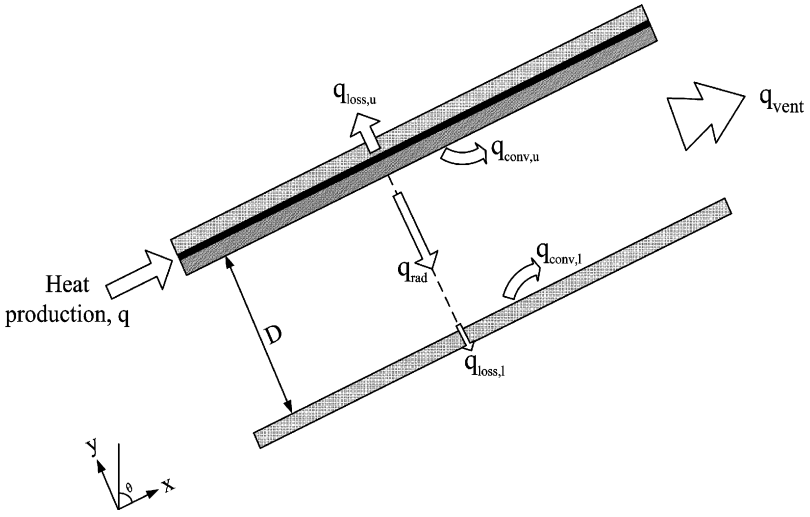

Fig. 10. Heat transfer modes in the cavity.

Table 1
Heat balance in ventilated roof cavity of inclination angle of 30°

Heat production (W/m^2)	Configuration	Opening (mm)		Total heat production (W)	Ventilation (W)	Top side loss (W)	Bottom side loss (W)	Deviation (W)	Portion of ventilation (%)	Portion of loss through top side (%)	Portion of loss through bottom side (%)	Portion of deviation (%)
		Inlet	Outlet									
150	Case A	78	78	275	103.0	155.6	8.4	8.0	38.5	58.2	3.2	3
			35		119.0	164.8	13.5	−22.3	40.8	54.6	4.6	−8
			20		98.3	164.4	20.2	−7.9	36.9	56.1	7.1	−3
			10		118.9	115.8	28.1	12.2	45.1	43.9	10.9	4
	Case B	78	78		103.0	155.9	8.6	7.5	38.5	58.2	3.2	3
		35			93.7	154.6	11.7	15.0	36.1	59.3	4.6	5
		20			50.6	156.2	16.8	51.3	22.2	70.0	7.8	19
		10			6.1	138.3	26.2	104.4	27.4	60.9	11.7	38
	Case C	78	78		103.0	155.9	8.6	7.5	38.5	58.2	3.2	3
		35	35		91.7	161.0	16.1	6.2	34.1	59.8	6.1	2
		20	20		96.0	162.0	23.5	−6.5	34.0	57.4	8.5	−2
		10	10		76.7	170.1	35.4	−7.2	27.1	60.2	12.8	−3
100	Case A	78	78	184	64.7	116.9	5.5	−3.1	34.7	62.4	3.0	−2
			35		85.7	126.3	9.9	−37.9	38.6	56.8	4.6	−21
			20		70.9	131.8	14.8	−33.4	32.5	60.5	7.0	−18
			10		70.2	128.9	18.8	−33.9	32.1	59.0	8.9	−18
	Case B	78	78		64.7	116.9	5.5	−3.1	34.7	62.4	3.0	−2
		35			80.1	124.0	14.0	−34.1	36.7	56.7	6.6	−19
		20			45.4	120.4	18.0	0.2	24.7	65.3	10.0	0
		10			9.9	123.7	19.7	30.7	6.5	80.6	13.0	17
	Case C	78	78		64.7	116.9	5.5	−3.1	34.7	62.4	3.0	−2
		35	35		65.5	121.8	10.8	−14.0	33.0	61.4	5.6	−8
		20	20		64.4	129.1	18.0	−27.4	30.3	60.9	8.8	−15
		10	10		50.6	133.7	26.5	−26.8	23.9	63.3	12.8	−15
75	Case A	78	78	138	57.6	101.9	7.1	−28.6	34.5	61.1	4.4	−21
			35		55.9	102.2	7.2	−27.4	33.8	61.7	4.5	−20
			20		42.8	112.4	12.4	−29.6	25.3	67.1	7.6	−21
			10		45.7	108.9	14.9	−31.6	26.8	64.0	9.2	−23
	Case B	78	78		57.6	101.9	7.1	−28.6	34.5	61.1	4.4	−21
		35			57.2	103.0	7.4	−29.6	34.1	61.3	4.6	−21
		20			41.5	103.7	10.0	−17.2	26.7	66.6	6.7	−12
		10			10.1	105.7	14.7	7.5	7.7	80.7	11.6	5
	Case C	78	78		57.6	101.9	7.1	−28.6	34.5	61.1	4.4	−21
		35	35		48.6	103.4	8.4	−22.4	30.3	64.3	5.4	−16
		20	20		44.5	105.7	13.4	−25.7	27.1	64.4	8.5	−19
		10	10		40.2	108.0	19.6	−29.8	23.9	64.2	12.0	−22
50	Case A	78	78	92	37.0	78.2	3.2	−26.5	31.2	65.8	3.0	−29
			35		35.5	84.2	4.7	−32.4	28.6	67.5	3.9	−35
			20		28.1	88.2	9.0	−33.3	22.3	70.3	7.4	−36
			10		29.4	83.9	9.4	−30.7	23.8	68.0	8.2	−33
	Case B	78	78		37.0	78.3	3.2	−26.6	31.2	65.8	3.0	−29
		35			34.5	80.4	5.4	−28.3	28.6	66.6	4.8	−31
		20			19.9	82.0	7.5	−17.4	18.1	74.8	7.1	−19
		10			7.4	80.8	9.6	−5.8	7.6	82.4	10.0	−6
	Case C	78	78		37.0	78.3	3.2	−26.6	31.2	65.8	3.0	−29
		35	35		30.7	84.2	6.1	−28.9	25.3	69.4	5.3	−31
		20	20		26.2	83.3	10.2	−27.7	21.8	69.4	8.8	−30
		10	10		18.2	84.1	12.5	−22.7	15.8	72.9	11.3	−25

only average values, representative of each case were presented in the following discussion.

4. Accuracy examination of the experiment

Heat transfer modes in the cavity were evaluated as shown in Fig. 10. When the heat q (W) was input to a heater plate, a part of the produced heat was released into ambient air through the upper structure of the heater as heat loss $q_{loss,u}$ (W). The rest of the produced heat was transferred to the upper surface of the cavity. The upper surface transferred heat to the cavity air through convection $q_{conv,u}$ (W) as well as to the lower surface of the cavity by radiation q_{rad} (W). When the lower surface of the cavity absorbed radiated heat, the temperature rose. The surface, in turn, transferred heat either to the cavity air by convection $q_{conv,l}$ (W) or into the ambient air through the lower structure as heat loss $q_{loss,l}$ (W). The temperature of air in the cavity rose after absorbing of the convection heat $q_{conv,u}$ and $q_{conv,l}$ from the upper and the lower surfaces, respectively. The heated air gained forcible buoyancy, and flowed upward. Heat q_{vent} was released out through the outlet while colder air continuously flowed into the cavity through the inlet. The heat q_{vent} could be expressed as

$$q_{vent} = \sum_{i=1}^{19} w\, c_p\, \rho\, V_{o,i}(T_{o,i} - T_\infty)\, \Delta y_i \quad (1)$$

where w (m) was the width of cavity, c_p (J/(kg K)) was the specific heat of cavity air, and ρ (kg/m^3) was the average air density at the outlet. In Eq. (1), the cavity flow was assumed to be parallel in all the layers. The depth of the cavity was divided into 19 thin layers of a thickness Δy_i (m) referring the 19 points of the velocity measurement. The air temperatures for every layer were

Table 2
Heat balance in ventilated roof cavity of inclination angle of 20°

Heat production (W/m^2)	Configuration	Opening (mm)		Total heat production (W)	Ventilation (W)	Top side loss (W)	Bottom side loss (W)	Deviation (W)	Portion of ventilation (%)	Portion of loss through top side (%)	Portion of loss through bottom side (%)	Portion of deviation (%)
		Inlet	Outlet									
150	Case A	78	78	275	100.7	167.5	7.6	−0.8	36.6	60.4	3.1	0
			35		111.5	173.0	13.0	−22.5	37.4	58.0	4.6	−8
			20		104.1	172.9	20.7	−22.7	34.9	58.0	7.1	−8
			10		–	–	–	–	–	–	–	–
	Case B	78	78		100.7	167.5	7.6	−0.8	36.6	60.4	3.1	0
		35			88.4	167.0	13.6	6.0	32.8	61.9	5.2	2
		20			51.4	165.4	17.2	41.0	22.0	70.3	7.7	15
		10			–	–	–	–	–	–	–	–
	Case C	78	78		100.7	167.5	7.6	−0.8	36.6	60.4	3.1	0
		35	35		93.4	175.0	17.4	−10.8	32.7	61.0	6.3	−4
		20	20		–	–	–	–	–	–	–	–
		10	10		–	–	–	–	–	–	–	–
100	Case A	78	78	184	74.2	86.7	6.7	16.4	44.2	51.5	4.3	9
			35		78.9	130.9	10.2	−36.0	35.9	59.4	4.7	−20
			20		68.9	132.9	15.4	−33.2	31.6	61.1	7.3	−18
			10		–	–	–	–	–	–	–	–
	Case B	78	78		74.2	86.7	6.7	16.4	44.2	51.5	4.3	9
		35			62.2	126.9	9.1	−14.2	31.4	63.8	4.8	−8
		20			38.3	124.5	11.9	9.3	21.9	71.0	7.1	5
		10			28.8	126.3	15.2	13.7	16.9	74.1	9.0	7
	Case C	78	78		74.2	86.7	6.7	16.4	44.2	51.5	4.3	9
		35	35		62.7	130.4	12.0	−21.1	30.5	63.4	6.1	−11
		20	20		–	–	–	–	–	–	–	–
		10	10		–	–	–	–	–	–	–	–
75	Case A	78	78	138	53.3	106.0	4.9	−26.2	32.6	64.2	3.3	−19
			35		47.5	110.0	7.1	−26.6	28.8	66.6	4.6	−19
			20		48.4	110.7	10.5	−31.6	28.4	65.0	6.5	−23
			10		–	–	–	–	–	–	–	–
	Case B	78	78		53.3	106.0	4.9	−26.2	32.6	64.2	3.3	−19
		35			47.8	106.6	7.5	−23.9	29.7	65.5	4.9	−17
		20			25.4	105.4	9.0	−1.8	18.1	74.9	7.0	−1
		10			31.7	106.1	11.7	−11.5	21.1	70.8	8.1	−8
	Case C	78	78		53.3	106.0	4.9	−26.2	32.6	64.2	3.3	−19
		35	35		43.1	109.4	7.9	−22.4	26.7	68.0	5.3	−16
		20	20		–	–	–	–	–	–	–	–
		10	10		–	–	–	–	–	–	–	–
50	Case A	78	78	92	35.2	85.8	4.3	−33.3	28.1	68.4	3.6	−36
			35		33.5	85.5	4.8	−31.8	27.1	68.7	4.2	−35
			20		30.4	88.5	9.0	−35.9	23.7	69.1	7.2	−39
			10		–	–	–	–	–	–	–	–
	Case B	78	78		35.2	85.8	4.3	−33.3	28.1	68.4	3.6	−36
		35			30.7	84.5	4.3	−27.5	25.7	70.3	4.0	−30
		20			20.1	85.1	7.0	−20.2	17.8	75.6	6.5	−22
		10			25.5	84.9	7.5	−25.9	21.4	71.9	6.7	−28
	Case C	78	78		35.2	85.8	4.3	−33.3	28.1	68.4	3.6	−36
		35	35		28.7	84.9	5.3	−26.9	24.2	71.0	4.8	−29
		20	20		–	–	–	–	–	–	–	–
		10	10		–	–	–	–	–	–	–	–

calculated from the measured temperature profile by interpolation. The term $(T_{o,i} - T_\infty)$ was the rise in temperature of air in the ith layer.

Heat losses through the upper and lower structures, $q_{loss,u}$ and $q_{loss,l}$, were calculated from measured temperature differences and their overall heat transfer coefficients. Heat losses through the sidewalls were not considered because such areas were small and insulated and the temperature differences were negligible. Consequently, the balance of heat transfer in the cavity was expressed as the following equation:

$$q = q_{vent} + q_{loss,u} + q_{loss,l} \quad (2)$$

Tables 1 and 2 show the portions of heat balance in the cavity in experiments with inclination angles of 30° and 20°, respectively. A large portion of the produced heat was released to the outside through the upper structure. The lower structure released a small portion of the heat. The deviation, which was residual of the produced heat from which the three heat transmissions were subtracted, was 16% in average. The proportions were between −39 and 38% in all the experiments. The positive error meant that the actual heat production was larger than the total of heat transmissions and vice versa. These deviations were larger in experiments with lesser heat production. In experiments with the lesser heat production, the accuracy of the velocity measurements seemed insufficient.

Case C gave the largest resistance to the air flow in the cavity compared to the other two cases. However, this case is probably the most suitable model for practical roof cavities.

Fig. 11 shows plots for the air velocity in the cavity against the square root of the product of q_{vent}, inclination angles, as well as

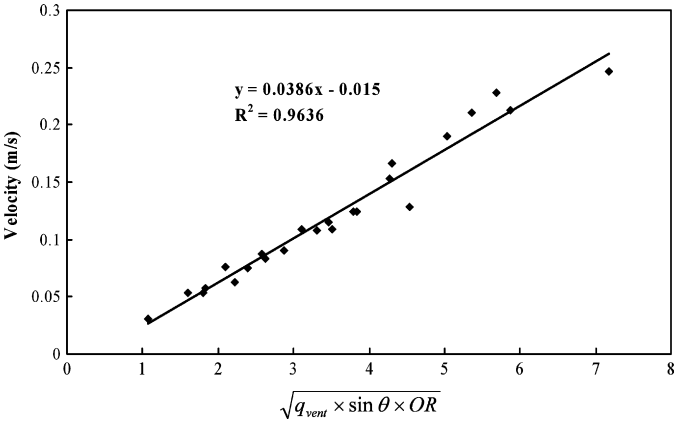

Fig. 11. Influence of inclination angles and opening ratios on velocity (case C).

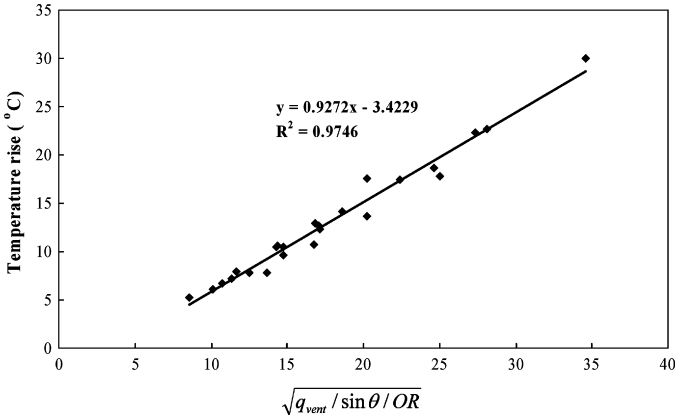

Fig. 12. Influence of inclination angles and opening ratios on temperature rise (case C).

opening ratios for case C. In this figure, the produced heat was represented by q_{vent}, since it was the same as transferred heat from the heated surfaces. Application of the least square method to the plotted data of $\overline{V}$, q_{vent}, $\sin\theta$, and OR had yielded:

$$\overline{V} = 0.039\left(\sqrt{q_{vent} \times \sin\ \theta \times OR}\right) - 0.015, \quad R^2 = 0.9636 \tag{3}$$

where $\overline{V}$ (m/s) was the average air velocity in the cavity. Eq. (3) indicated that the induced air velocity in the cavity was proportional to the square root of the buoyant pressure. In this study, the buoyant pressure was expressed by the term $q_{vent} \times \sin\theta$ while OR simulated deformation resistances in the cavity where the two terms opposed each other in order to dictate induced velocity in the cavity. The coefficients of determination R^2 were 0.9626, 0.9553, and 0.9636 for cases A, B, and C, respectively.

Fig. 12 shows the influence of inclination angles and opening ratios on the temperature rise for case C. With the least square method applied to the data in the figure, the obtained correlation was

$$\overline{T} = 0.927\left(\sqrt{\frac{q_{vent}}{\sin\ \theta/OR}}\right) - 3.423, \quad R^2 = 0.9746 \tag{4}$$

where $\overline{T}$ (°C) was the average temperature rise in the cavity outlet. All the plots exhibited an ideal concentration in this figure. Eq. (4) indicated that in case of temperature rise in the cavity, resistance of the air flow correlated inversely to the square root of the sine component of inclination angles and opening ratios.

The coefficients of determination R^2 were 0.9359, 0.0993, and 0.9746 for cases A, B, and C, respectively. The coefficients of determination for cases A and C were satisfactory hence the experiment seemed reliable in these two cases. However, in case B, the coefficient of determination was very small. It might mean that the behavior of heat and air flow was uncertain in this case. It was presumed that a secondary counter flow took place at the top opening because of the larger outflow there, but there was not enough air supplied from the bottom opening in this configuration. This description might indicate that the heat transfer was disturbed by the air, which entered from the top opening and recirculated in the cavity.

In the research conducted by Nada and Moawed [19], it was reported that when the inclination angles of the enclosure increased from 90° to 180°, in which the location of the heated surface was the same to the present experiment, the effect of opening ratio on the heat transfer rate in the cavity decreased.

Table 3
Reynolds number for all cases with a heat production of 150 W/m^2

Inclination angle	Experimental cases	Opening size (mm)		Opening ratio	Average velocity	Reynolds number
		Inlet	Outlet			
30°	Fully open	78	78	1.00	0.25	2009
	A	78	35	0.45	0.19	1534
		78	20	0.26	0.12	987
		78	10	0.13	0.11	908
	B	35	78	0.45	0.16	1327
		20	78	0.26	0.07	530
		10	78	0.13	0.01	43
	C	35	35	0.45	0.13	1050
		20	20	0.26	0.11	889
		10	10	0.13	0.06	511
20°	Fully open	78	78	1.00	0.21	1738
	A	78	35	0.45	0.17	1353
		78	20	0.26	0.12	980
		78	10	0.13	–	–
	B	35	78	0.45	0.15	1231
		20	78	0.26	0.06	520
		10	78	0.13	–	–
	C	35	35	0.45	0.12	1014
		20	20	0.26	–	–
		10	10	0.13	–	–

5. Reynolds number

Table 3 shows the corresponding Reynolds number for various cases with a heat production of 150 W/m^2. With OR 1.0, Reynolds numbers were 2009 and 1738 for inclination angles of 30° and 20°, respectively. With OR 0.45 in case C, the Reynolds number decreased to 1050 and 1014, respectively. With natural ventilation through a roof cavity, the flow seemed to be laminar judging from the Reynolds numbers.

6. Conclusions

This paper presented the characteristics of the air flow in an inclined heated cavity model under steady condition in a laboratory. The main findings were as follows.

The surface temperature was low but it arose quickly in the inlet region. In the outlet region, the surface temperature rise was gentle. The surface temperature change was not linear along the flow. The effect of the opening ratio was essential for the thermal behavior of air flow in the cavity.

The air temperature was high in the direct vicinity to the upper surface. It decreased rapidly with the distance from the heated surface.

The velocity profiles showed a complicated shape reflecting the temperature profiles. The highest velocity appeared in the near region to the heated surface. The highest velocity was 0.32 m/s, and average velocity was 0.25 m/s in the case when a heat production was 150 W/m^2, both openings were fully opened, and an angle of 30°.

The velocity was high when the heat production was high. This is a favourable character of natural ventilation to dissipate solar heat in its high intensity.

The flow resistance was simulated by placing slits at the inlet and/or outlet of the cavity. The higher resistance caused low velocity and high temperature rise. When OR was reduced to 45%, the average velocity changed from 0.25 to 0.13 m/s, and the air temperature arose from 10.6 to 17.5 °C in the same case.

When the angle was changed from 30° to 20°, with a heat production was still kept at 150 W/m^2 and both openings fully open, the air velocity decreased from 0.25 to 0.21 m/s.

The highest Reynolds number in the experiment was 2009. This indicated that the flow in the cavity belonged to laminar region.

The average air velocity of 0.13 m/s of OR 45% case corresponded to a ventilation number of 96 times/h. The roof cavity ventilation appeared to be effective in solar incidence evacuation before it was transferred to the lower roof structure and then further down into the space below when the cavity and the openings were arranged to optimally utilize the natural force of buoyancy of the air in the cavity. This suggests that natural ventilation in the roof cavity can be effectively applied in reducing the cooling load of a factory building.

Acknowledgement

This study was supported in part by the 21st century COE Program "Ecological Engineering for Homeostatic Human Activities", from the Ministry of Education, Culture, Sports, Science and Technology, Japan.

References

[1] J. Khedari, J. Hirunlabh, T. Bunnag, Experimental study of a roof solar collector towards the natural ventilation of new houses, Energy and Buildings 26 (1997) 159–164.
[2] J. Khedari, W. Mansirisub, S. Chaima, N. Pratinthong, J. Hirunlabh, Field measurements of performance of roof solar collector, Energy and Buildings 31 (2000) 171–178.
[3] J. Hirunlabh, S. Wachirapuwadon, N. Pratinthong, J. Khedari, New configurations of a roof solar collector maximizing natural ventilation, Building and Environment 36 (2001) 383–391.
[4] J. Khedari, B. Boonsri, J. Hirunlabh, Ventilation impact of a solar chimney on indoor temperature fluctuation and air change in a school building, Energy and Buildings 32 (2000) 89–93.
[5] X.Q. Zhai, Y.J. Dai, R.Z. Wang, Comparison of heating and natural ventilation in a solar house induced by two roof solar collectors, Applied Thermal Engineering 25 (2005) 741–757.
[6] B. Moshfegh, M. Sandberg, Flow and heat transfer in the air gap behind photovoltaic panels, Renewable and Sustainable Energy Reviews 2 (1998) 287–301.
[7] M. Sandberg, B. Moshfegh, Ventilated solar roof air flow and heat transfer investigation, Renewable Energy 15 (1–4) (1998) 287–292.
[8] X.Q. Zhai, Y.J. Dai, R.Z. Wang, Experimental investigation on air heating and natural ventilation of a solar air collector, Energy and Buildings 37 (2005) 373–381.
[9] M. Manzan, O. Saro, Numerical analysis of heat and mass transfer in a passive building component cooled by water evaporation, Energy and Buildings 34 (2002) 369–375.
[10] M. Ciampi, F. Leccese, G. Tuoni, Energy analysis of ventilated and microventilated roofs, Solar Energy 79 (2) (2005) 183–192.
[11] J.N. Arnold, I. Catton, D.K. Edwards, Experimental investigation of natural convection in inclined rectangular regions of differing aspect ratio, Transactions of ASME, Journal of Heat Transfer, Series C 98 (1976) 67–71.
[12] J. Khedari, P. Yimsamerjit, J. Hirunlabh, Experimental investigation of free convection in roof solar collector, Building and Environment 37 (2002) 455–459.
[13] W. Puangsombut, J. Hirunlabh, J. Khedari, B. Zeghmati, M.M. Win, Enhancement of natural ventilation rate and attic heat gain reduction of roof solar collector using radiant barrier, Building and Environment 42 (2007) 2218–2226.
[14] L.F.A. Azevedo, E.M. Sparrow, Natural convection in open-ended inclined channels, Journal of Heat Transfer 107 (1985) 893–901.
[15] Z.D. Chen, P. Bandopadhayay, J. Halldorsson, C. Byrjalsen, P. Heiselberg, Y. Li, An experimental investigation of a solar chimney model with uniform wall heat flux, Building and Environment 38 (2003) 893–906.
[16] M. Sandberg, B. Moshfegh, The investigation of fluid flow and heat transfer in a vertical channel heated from one side by PV elements. Part II. Experimental study, in: Proceedings of the Fourth Renewable Energy Congress, Denver, CO, (1996), pp. 254–258.
[17] T. Bunnag, J. Khedari, J. Hirunlabh, B. Zeghmati, Experimental investigation of free convection in an open-ended inclined rectangular channel heated from the top, International Journal of Ambient Energy 25 (3) (2004) 151–162.
[18] N. Katsoulas, T. Bartzanas, T. Boulard, M. Mermier, C. Kittas, Effect of vent openings and insect screen on greenhouse ventilation, Biosystem Engineering 93 (4) (2006) 427–436.
[19] S.A. Nada, M. Moawed, Free convection in tilted rectangular enclosures heated at the bottom wall and vented by different slots-venting arrangements, Experimental Thermal and Fluid Science 28 (2004) 853–862.
[20] P.H. Biwole, M. Woloszyn, C. Pompeo, Heat transfers in a double-skin roof ventilated by natural convection in summer time, Energy and Buildings 40 (2008) 1487–1497.